Solar Energy, Vol. 18, pp. 113–127. Pergamon Press 1976. Printed in Great Britain

A DESIGN PROCEDURE FOR SOLAR HEATING SYSTEMS†

S. A. KLEIN, W. A. BECKMAN and J. A. DUFFIE
University of Wisconsin, Madison, WI 53706, U.S.A.

(*Received* 21 *July* 1975; *in revised form* 17 *November* 1975)

Abstract—This paper is concerned with the design of solar space and water heating systems for residences. A simulation model capable of estimating the long-term thermal performance of solar heating systems is described. The amount of meteorological data required by the simulation in order to estimate long-term performance is investigated. The information gained from many simulations is used to develop a general design procedure for solar heating systems. The result is a simple graphical method requiring monthly average meteorological data which architects and heating engineers can use to design economical solar heating systems. A method of estimating the monthly average radiation on tilted surfaces is given in the Appendix.

INTRODUCTION

Simulations of solar processes can serve three distinct purposes. First, they provide a means of analyzing the dynamic performance of a specified system in response to selected meteorological data. Analyses of this type can be used for a variety of purposes such as to investigate various control strategies, to determine system temperature extremes, and to gain an understanding of the dynamic relationships between system components. Second, simulations can be used directly as a design tool for particular applications. The use of simulations for this purpose is often warranted for the design of large or complex systems, such as for the heating systems of institutional buildings.

Third, simulation methods can be used for generalized design studies. The results of many simulations can be used to develop generalized performance charts which correlate the performance of a particular type of system with its design parameters and the weather. This paper is concerned with this third purpose as it applies to solar space and water heating systems for residences using liquid heat transfer fluids.

The paper is divided into three parts. The first describes and justifies simplifications of existing models of solar heating system components which constitute a simulation model capable of estimating the long-term thermal performance of a specified system at reasonable computing cost. The second part is concerned with the problem of determining the amount of meteorological data required by the simulation in order to estimate long-term system performance. The third part uses information gained from many simulations to develop a general design procedure for solar heating systems. The result is a simple graphical method by which architects and heating engineers can design economical liquid-based solar heating systems for residences.

PART I. DEVELOPMENT OF A SIMULATION MODEL

I.1 *Description of the solar heating system*

A schematic diagram of the solar heating system is shown in Fig. 1. The system considered uses liquids, either water or antifreeze solution, as the energy transfer and storage mediums.

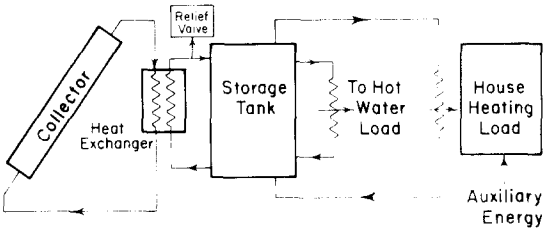

Fig. 1. Schematic of a solar space and water heating system.

A flat-plate collector is used to transform incident solar radiation into thermal energy. This energy is stored in the form of sensible energy and used as needed to supply the space and water heating loads. An antifreeze solution is generally circulated through the collector to avoid the problems of freezing and corrosion. A heat exchanger is used between the collector and the tank because it is generally more economical than using the antifreeze solution as the energy storage medium. A second heat exchanger is used to transfer energy from the main storage tank to the smaller domestic hot water tank. Conventional auxiliary heaters are provided to supply energy for both the space and water heating loads when the energy in the storage tank is depleted. Controllers, relief valves, pumps and piping make up the remaining equipment.

I.2 *The simulation method*

A simulation model of a solar heating system is developed by interconnecting mathematical models of each of the system components. Properly formulated, the simulation model provides an estimation of the performance of a system much more quickly and cheaply than is possible by experiment.

Computational simplicity in a simulation model used for these generalized design studies is needed to allow an examination of the long-term performance of many system designs in a variety of climates at reasonable computing cost. Here, long-term is defined to be a period of time sufficient to describe the performance of heating systems in a climate, generally a period of one or more years. Details in the component models (from which the system model is formulated) having only a small effect

†Presented at the 1975 I.S.E.S. International Solar Energy Congress and Exposition, Los Angeles, California (28 July–1 Aug. 1975).

upon the long-term system performance are excluded. Modelling simplifications of this type have developed from experience with TRNSYS[1], a general simulation program for solar energy systems.

I.3 *Energy collection*

The flat-plate collector, the collector-tank heat exchanger, the pressure relief valves, the circulation pumps and the pump controller are all involved in energy collection and transfer to the storage tank. Mathematical models describing the thermal performance of each of these components can be formulated and combined into a single model which describes the combined thermal performance of all of these components in a computationally efficient manner.

The Hottel and Whillier[2] collector equation is useful because of its computational efficiency and excellent agreement with more elaborate models[3]. The model expresses the rate of energy collection Q_u in the form

$$Q_u = F_R A[H_T(\tau\alpha) - U_L(T_i - T_a)] = (\dot{m}C_p)_c(T_0 - T_i) \tag{1}$$

where

$$F_R = \frac{(\dot{m}C_p)_c}{AU_L}\left[1 - \exp\left(\frac{-F'U_L A}{(\dot{m}C_p)_c}\right)\right]. \tag{2}$$

Measurements of H_T, the radiation incident on the tilted collector surface, are generally unavailable. As a result, H_T must be estimated from measurements of H, the radiation incident on a horizontal surface, available in the form of hourly or daily totals for many locations throughout the United States.

Several methods of relating H_T to H have been proposed, none of which are entirely satisfactory. The method adopted here[4, 5] expresses H_T as

$$H_T = H_b R_b + H_d(1 + \cos s)/2 + \rho(H_b + H_d)(1 - \cos s)/2 \tag{3}$$

where H_b and H_d are respectively the rates of beam and diffuse radiation incident on a horizontal surface; R_b is the ratio of beam radiation on a tilted surface to that on a horizontal surface. If the tilted surface is oriented directly towards the equator, then

$$R_b = \frac{\cos(\phi - s)\cos\delta\cos\omega + \sin(\phi - s)\sin\delta}{\cos\phi\cos\delta\cos\omega + \sin\phi\sin\delta} \tag{4}$$

ρ is the ground reflectance. Liu and Jordan[5] suggest that ρ should be 0.2 when there is no snow and 0.7 when there is snow cover.

The difficulty in using eqn (3) is that measurements of H_b and H_d are generally unavailable. However, H_b and H_d can be estimated at hourly intervals from a knowledge of the daily total radiation on a horizontal surface using the results of Liu and Jordan[6]. Figure 7 in Liu and Jordan is used to estimate the daily diffuse radiation as a function of K_T, the ratio of daily total radiation on a horizontal surface to the extraterrestrial radiation. Then the hourly diffuse and total radiation on a horizontal surface are estimated from the daily diffuse and total radiation using the relationships given in Figs. 15 and 16 of Liu and Jordan[6].

The basic problem in estimating H_T in this manner is that the hourly fluctuations of H_T caused by clouds cannot be represented. Although the daily total radiation may vary from day to day, the distribution of the radiation throughout each day is assumed to have the shape of the long term average, a function of latitude and time of year.

Despite this problem, the use of this method of estimating H_T can be justified in several ways. Close[7] suggested that the overall performace of solar heating systems of the type considered here is not particularly sensitive to the distribution of radiation during the day, although the daily total radiation is important. Also, the use of the smooth long-term average distribution of the hourly radiation always results in a conservative estimate of system performance. The estimate is most conservative for system designs which provide a large fraction of the total heating load in a climate which typically has large fluctuations in the radiation intensity throughout the day.

The $(\tau\alpha)$ product is a function of the angle of incident (beam and diffuse) radiation as shown in Duffie and Beckman[4]. The angular dependence has been included in the model so that the effect of collector orientation can be assessed.

The collector geometry efficiency factor F', a function of the collector construction, can be determined in the manner given by Whillier[8] or Bliss[9]. The overall energy loss coefficient U_L is a complicated function of both the collector construction and its operating conditions. Klein[10] has developed an expression which approximates this function in closed form.

Neglecting the dependence of U_L upon operating conditions provides one means of simplifying the simulation model. An examination of plots of U_L vs temperatures and windspeed indicates that the functional dependence of U_L upon the operating conditions is not very strong, particularly for collectors with two or more transparent covers and/or with selective plate surfaces. The effect of U_L on the long-term performance of a solar heating system of the type shown in Fig. 1 has been examined for a variety of system designs and operating conditions. It has been found that, for a collector with two glass covers and a non-selective plate surface, the error in the percent of the total heating load supplied by solar energy caused by neglecting the dependence of U_L upon operating conditions is generally no more than 5 per cent. Provided that the value of U_L is evaluated at the estimated average collector operating conditions, the error can be quite small. The dependence of U_L upon fluctuating operating conditions has been neglected in the generalized design studies described below.

In the system shown in Fig. 1, the temperature of the fluid entering the collector T_i is the temperature of the fluid at the outlet of the heat exchanger in the collector–heat exchanger flow circuit (neglecting thermal losses in piping). The thermal performance of the heat exchanger with constant effectiveness ϵ_c can be expressed[11] as

$$Q_{hx} = \epsilon_c(\dot{m}C_p)_{\min}(T_0 - T) = (\dot{m}C_p)_s(T_1 - T) \tag{5}$$

where T is the temperature of the water at the bottom of the storage tank; $(\dot{m}C_p)_{\min}$ is the minimum of $(\dot{m}C_p)_c$ and $(\dot{m}C_p)_s$.

If, as suggested by de Winter[12], a quasi steady-state condition is assumed so that Q_u, the rate at which energy is collected, equals Q_{hx}, the rate at which energy is transferred across the collector-tank heat exchanger, then eqns (1) and (5) can be reduced to a single equation of the form

$$Q_u = F'_R A[H_T(\tau\alpha) - U_L(T - T_a)] \tag{6}$$

where

$$F'_R/F_R = \left\{1 + \left[\frac{F_R U_L A}{(\dot{m}C_p)_c}\right]\left[\frac{(\dot{m}C_p)_c}{\epsilon_C(\dot{m}C_p)_{\min}} - 1\right]\right\}^{-1}. \tag{7}$$

de Winter defines F'_R/F_R to be the "heat exchanger factor", an index between 0 and 1 which indicates the penalty in energy collection imposed by the use of a double flow circuit.

Equation (6) applies when fluid is being pumped through the collector–exchanger and exchanger–tank flow circuits and a positive energy gain is being achieved. The relief valve ensures that T_1, the temperature of the water leaving the heat exchanger, does not exceed the boiling point $T_{\max}$. At night, or during periods of low radiation, the energy gain becomes zero or negative and the pumps must be turned off. Close[7] has shown that the best (i.e. highest energy collection) control strategy for pump operation is achieved by the use of an on-off differential controller monitoring T, the temperature of the fluid at the bottom of the storage tank, and T_0, the fluid temperature in the outlet manifold of the collector. A model which expresses Q_d, the rate at which energy is transferred to the storage tank, in terms of the combined thermal performance of the collector, the heat exchanger (for double flow circuit systems), the controller, and the relief valve can be written†

$$Q_d = \begin{cases} F'_R A[H_T(\tau\alpha) - U_L(T - T_a)]^+ & \text{if } T_1 \le T_{\max} \\ (\dot{m}C_p)_s(T_{\max} - T) & \text{otherwise} \end{cases} \tag{8}$$

I.4 *Energy storage*

Collected solar energy, in the form of heated water, is stored in two tanks, a large main tank and a smaller domestic water tank. Energy is transferred from the main to the domestic water tank when the temperature of the water in the domestic water tank falls below that in the main tank.

The thermal performance of the energy storage components of the system shown in Fig. 1 can be described by formulating models of both tanks, the heat exchanger, the pumps and the pump controller. However, such a complicated model is often unnecessary. The average temperature of the domestic water tank over an extended period is very nearly the same as that of the main storage tank, provided that the heat exchanger between the two tanks is adequate. For present purposes it is sufficiently accurate to model energy storage as a single tank which has a volume equal to the sum of the volumes of the main and domestic water tanks.

The basic heat and mass transfer relations governing the storage tank behavior are complicated. However, according to Close[7], thermally stratified storage can be modelled by considering the tank to consist of N fully-mixed segments. The model assumes that the fluid entering the tank seeks the tank segment to which it is closest to in density, and thus temperature. This assumption is reasonable when the fluid flows into and out of the tank are at very low velocities, a condition which minimizes mixing. The temperature of each of the N fully-mixed segments is determined by the numerical integration of its time derivative, which is described by an energy balance about the segment[4, 7, 13].

In order to assess the effects of thermal stratification on the overall perfomance of these systems, the results of long-term simulations using models of both stratified and fully-mixed energy storage tanks have been compared for systems of several different designs supplying 20–85 per cent of the total heating load with solar energy. It has been found that thermal stratification increases the fraction of the total heating load supplied by solar energy by only 1–3 per cent. (Systems supplying a larger fraction of the total heating load were able to benefit more from stratification effects than were systems supplying smaller fractions since system temperatures were higher for these system designs.) Since the effects of thermal stratification are relatively small and a fully-mixed tank model provides a conservative estimate of system performance, a fully-mixed tank model has been used in the generalized design studies which follow. The model expresses the tank temperature in terms of its time derivative which is described by an energy balance about the tank.

$$MC_p\frac{dT}{dt} = Q_d - (Q_L - E_L) - (Q_w - E_w) \tag{9}$$

where Q_L is the space heating load; E_L is the auxiliary energy required in addition to solar energy in order to meet the space heating load; Q_w is the water heating load; E_w is the auxiliary energy required in addition to solar energy in order to meet the water heating load. Models for Q_L, E_L, Q_w and E_w will be developed in the following sections.

I.5 *Heating loads*

Many different models of the space heating energy requirements have been proposed, ranging in complexity from the simple quasi steady-state "energy per unit time per unit temperature difference" model to, for example, the very detailed transient model developed by ASHRAE[14]. A variety of factors influence heating requirements such as the location of the building, its architectural design, orientation and construction quality, and the particular habits of the occupants. The results of a survey conducted by Grot[15] indicate that there is a large variation in energy usage, even for residences of identical

†The + superscript indicates that only positive values are to be considered.

construction in the same location. It seems that the use of elaborate models of space heating energy requirements may not be justified here.

A simple space heating load model, the energy per degree-time model, expresses the heating load Q_L as a linear function of the difference between the inside temperature of the building (reduced to account for internal energy generation) and the ambient temperature.

$$Q_L = UA(T_r - T_a)^+. \tag{10}$$

The constant UA is the space heating load at design conditions (estimated in the manner described by ASHRAE[16]) divided by the design temperature difference.

The total heating load over an extended period, estimated by eqn (10) should be nearly identical to the estimations provided by more elaborate models if UA is properly chosen. The difficulty with the energy per degree-time model is that it may incorrectly predict the time distribution of the heating load because it does not directly account for heating gains as a result of fenestration or the thermal capacitance effects of the building.

The effect of load distribution upon the performance of solar water heating systems has been examined by Gutierrez *et al.*[13] by comparing the performance of systems in which a specified daily energy load was imposed at the "least favorable" time (i.e. early morning) with that in which the load was at the "most favorable" time (i.e. early afternoon). For systems with a storage capacity of 90 kg of water per square meter of collector area, the effect of load distribution on the percent of the total load supplied by solar energy over a 30-day period was about 5 per cent. This effect was somewhat larger for systems with smaller energy storage capacities.

The difference between the load distributions estimated by the energy per degree-time and more elaborate models would probably not be as extreme as the difference between the least and most favorable load distributions examined in the Gutierrez study. The effect of load distribution estimated by Gutierrez can probably be considered to be an upper limit. With this justification, the energy per degree-time model has been used in the simulation.

An accurate model of the water heating load cannot be formulated in general since it is highly dependent upon the particular habits of the occupants. An average hot water demand, a function of the time of day and family size, has been established[17]. The domestic water load can be modelled as

$$Q_w = (\dot{m}C_p)_w[T_w - T_m] \tag{11}$$

where T_w is the minimum acceptable hot water temperature, generally about 60°C and T_m is the temperature of available mains supply. As just noted, the time distribution of the water heating load will have only a small effect upon the long-term system performance (particularly if the water heating load is small relative to the space heating load).

I.6 *Auxiliary energy*

The system shown in Fig. 1 uses two auxiliary heaters. One heater adds auxiliary energy whenever the temperature of the water required for domestic use falls below the minimum acceptable temperature T_w. The rate at which energy is supplied by this auxiliary heater E_w can be modelled simply as

$$E_w = (\dot{m}C_p)_w[T_w - T]^+. \tag{12}$$

The second auxiliary heater supplies energy for space heating whenever the solar energy is insufficient to meet the space heating load. In practice, this condition is detected by a thermostat monitoring the temperature within the building. The use of the energy per degree-time space heating model, however, assumes that the temperature within the building is constant; thus it cannot be used in the system model to indicate that auxiliary energy is required. Instead, the model assumes that auxiliary energy is supplied whenever the rate at which solar energy can be provided, Q_{max}, is less than Q_L. Q_{max} can be expressed in terms of the effectiveness of the crossflow heat exchanger which transfers energy from the water in the main storage tank to the air within the building as in eqn (13).

$$Q_{max} = \epsilon_L C_{min}(T - T_R). \tag{13}$$

The rate at which auxiliary energy supplements the space heating load is then

$$E_L = [Q_L - Q_{max} - (UA)_s(T - T_{env})]^+. \tag{14}$$

Equation (14) assumes that the tank energy losses reduce the space heating load.

C_{min}, the minimum of the two fluid flow capacitances through the heat exchanger, will generally be that of the air. The dimensionless parameter $\epsilon_L C_{min}/UA$ provides a measure by which the crossflow heat exchanger for a specified building can be sized. It will be shown below that the reduction in system performance due to too small a heat exchanger will be appreciable for values of $\epsilon_L C_{mn}/UA$ less than 1. Reasonable values of $\epsilon_L C_{min}/UA$ for solar space heating systems are between 1 and 3.

PART II. USE OF METEOROLOGICAL DATA

The component models described in Part I collectively form a simulation model of a solar space and water heating system using liquid heat transfer fluids. The simulation model will provide an estimate of the system performance in the location of interest for the period over which meteorological data is supplied. The difficulty in using simulation methods for design, however, extends beyond the development of a simulation model; meteorological data sufficient to characterize long-term system performance must be available. For design, "long term" refers to a period equivalent to or representative of the expected life of the system, which may be 10–20 years.

The problem of determining the amount of meteorological data needed to estimate long-term performance has received relatively little attention. Hottel and Whillier[2] used 3 years of data in the construction of their utilizability curves, although they conceded that ten years' data would provide a better statistical picture. In

extending the utilizability curves, Liu and Jordan[5] noted that the amount of meteorological data needed to describe the long-term performance of a collector is location dependent. They used 5 years of data to construct the generalized utilizability curves, adding that "substantial error can and does occur when data of a finite number of years are used to predict the long-term average performance of a collector". Surprisingly, the more recent computer simulation studies[18–21] have used no more than 1 year of data (primarily because of the computing effort involved in simulating system performance for longer periods), although an "average" or "typical" year was generally used in these studies. The definition of an "average" year remains uncertain, although Beseman[22] has proposed one definition in regard to solar radiation data.

The adequacy of using an "average" or "typical" year of meteorological data with a simulation model to provide an estimate of the long-term system performance depends on the sensitivity of system performance to the hourly and daily weather sequences. Regardless of how it is selected, an "average" year cannot be expected to have the same weather sequences as those occurring in the long term. However, the simulated performance of a system for an "average" year may provide a good estimate of the long-term system performance if the weather sequences occurring in the average year are representative of those occurring in the long term or if the system performance is independent of the weather sequences.

To investigate the possibility of using an "average" year to provide an estimate of the long-term system performance, the simulated performance of four systems calculated at half hourly intervals has been examined for a period of 8 years using meteorological data for Madison, Wisconsin. The average performance of each system for the 8-year period has been compared with the performance calculated for an average year. The average year was construced by selecting, for each month of the year, that month of data from the 8-year period which most closely corresponded to the average monthly insolation and ambient temperature. The meteorological conditions for the heating season months of the 8 years are given in Tables 1 and 2. The circled entries identify the months chosen for the "average" year. Table 3 identifies the design parameters of the four systems. The simulated performance of the four systems expressed as the fraction of the heating load supplied by solar energy for each month of the 8 years and for the average year appear in the upper part of Tables 4–7.

An examination of the year load fractions supplied by solar energy for each of the 8 years shows that the system performance does vary from one year to the next as expected. However, the year to year variability of system performance is not the issue in question but rather whether or not the system performance calculated for the "average" year provides a reasonable estimate of the average system performance for the 8-year period.

The 8-year averages of the monthly load fractions supplied by solar energy for system *A*, a system which supplies a relatively small fraction of the total heating load, are reasonably close to those calculated for the average year for all months in which there is a significant heating load. However, as the system size is increased for systems *B*, *C* and *D*, respectively, the differences between the 8-year averages and the "average" year values increase. An explanation which can be offered to account for this behavior is that the sequences of weather are more important to a system which supplies a large

Table 1. Monthly solar radiation incident on a 45 surface in Madison, Wisconsin kJ m^{-2} × 10^{-6}

	Sep.	Oct.	Nov.	Dec.	Jan.	Feb.	Mar	Apr.	May	Total
1948–49	0.61	0.54	0.23	0.36	0.29	0.50	0.51	0.60	0.57	4.20
1949–50	0.55	0.54	(0.34)	(0.30)	0.34	0.44	0.50	0.48	0.60	4.09
1950–51	0.55	0.50	0.37	0.37	0.40	0.37	0.48	0.41	0.57	4.01
1951–52	(0.55)	0.42	0.39	0.26	0.28	0.41	0.54	0.52	0.49	3.87
1952–53	0.64	0.59	0.38	0.22	0.23	0.38	0.48	0.46	(0.50)	3.87
1953–54	0.68	0.55	0.38	0.26	(0.33)	0.41	(0.53)	0.52	0.55	4.21
1954–55	0.49	0.37	0.27	0.22	0.32	(0.46)	0.60	0.57	0.64	3.94
1955–56	0.61	(0.45)	0.31	0.27	0.37	0.50	0.57	(0.54)	0.49	4.11
8-yr Average	0.58	0.50	0.33	0.28	0.32	0.43	0.53	0.51	0.55	4.04
Std. Dev.	0.09	0.10	0.09	0.09	0.09	0.08	0.08	0.09	0.09	0.14

Table 2. Monthly space and water heating loads kJ × 10^{-6}

	Sep.	Oct.	Nov.	Dec.	Jan.	Feb.	Mar.	Apr.	May	Total
1948–49	3.85	9.76	13.07	20.38	21.52	23.72	17.77	11.60	5.78	127.45
1949–50	5.85	7.15	(14.99)	(20.62)	21.71	23.33	19.75	14.27	6.75	134.43
1950–51	4.68	7.44	17.17	25.00	24.28	24.52	19.13	12.95	5.25	140.43
1951–52	(5.56)	9.00	19.35	22.90	22.31	20.38	19.61	10.89	6.06	136.08
1952–53	4.77	11.58	13.35	19.91	21.05	21.07	17.03	12.92	(7.04)	128.73
1953–54	4.77	7.24	13.30	19.31	(23.27)	17.60	(17.86)	10.36	8.16	121.89
1954–55	4.30	8.82	14.53	20.53	23.07	(23.19)	18.59	8.24	4.99	126.27
1955–56	4.58	8.30	17.42	23.42	22.73	22.40	18.97	(12.40)	7.88	138.10
8-yr Average	4.79	8.66	15.40	21.51	22.50	22.03	18.59	11.71	6.49	131.67
Std. Dev.	0.64	1.50	2.32	2.00	1.06	2.25	0.96	1.87	1.17	6.51

Table 3. System design parameters

A	20 m² (System A) 40 m² (System B) 80 m² (System C) 100 m² (System D)
$(\dot{m}C_p)_c/A$	210 kJ hr^{-1} C^{-1} m^{-2}
M/A	75 kg (H_2O) m^{-2}
F'_R	0.90
U_L	15.0 kJ hr^{-1} C^{-1} m^{-2}
$(\tau\alpha)_n$	0.80
s	45°
UA	1200 kJ hr^{-1} C^{-1}
D	280 kg (H_2O) day^{-1}
$\epsilon_L C_{min}/UA$	2

fraction (but less than all) of the total heating load than for one which supplies a smaller fraction. The larger system is capable of more fully charging the storage tank during favorable weather. If such weather continues, the larger system will collect additional energy at a lower efficiency (because of the high storage tank temperature), and it may have to "dump" energy when the tank becomes fully charged depending upon the weather sequences which follow.

On a month-by-month basis, significant differences can be found between the 8-year average and the average year load fractions supplied by solar energy, although the largest differences generally occur for months in which

Table 4. Fraction of the heating load supplied by system A

	Sep.	Oct.	Nov.	Dec.	Jan.	Feb.	Mar.	Apr.	May	Average
Calculated from the simulation										
1948–49	0.97	0.57	0.16	0.16	0.11	0.19	0.27	0.50	0.81	0.29
1949–50	0.80	0.73	0.21	0.13	0.14	0.17	0.23	0.32	0.73	0.27
1950–51	0.66	0.88	0.21	0.13	0.14	0.12	0.23	0.28	0.79	0.25
1951–52	0.81	0.45	0.19	0.09	0.10	0.18	0.26	0.41	0.62	0.25
1952–53	0.91	0.55	0.28	0.09	0.08	0.15	0.26	0.33	0.57	0.26
1953–54	0.96	0.69	0.30	0.11	0.12	0.22	0.28	0.48	0.57	0.30
1954–55	0.81	0.45	0.17	0.08	0.11	0.18	0.31	0.65	0.88	0.27
1955–56	0.94	0.50	0.16	0.09	0.14	0.21	0.29	0.43	0.52	0.26
8-yr Average	0.86	0.60	0.21	0.11	0.12	0.18	0.27	0.42	0.69	0.27
Average year	0.81	0.50	0.20	0.13	0.12	0.18	0.28	0.43	0.60	0.27
Estimated from the performance chart										
1948–49	1.00	0.53	0.14	0.16	0.11	0.21	0.29	0.51	0.81	0.29
1949–50	0.78	0.68	0.21	0.12	0.14	0.19	0.26	0.34	0.77	0.28
1950–51	0.62	0.89	0.21	0.13	0.15	0.14	0.25	0.31	0.85	0.26
1951–52	0.81	0.45	0.19	0.09	0.10	0.20	0.29	0.47	0.69	0.26
1952–53	0.97	0.51	0.27	0.07	0.07	0.16	0.29	0.36	0.64	0.27
1953–54	1.00	0.68	0.27	0.10	0.12	0.23	0.31	0.49	0.63	0.31
1954–55	0.85	0.40	0.15	0.06	0.12	0.19	0.34	0.64	0.95	0.27
1955–56	0.96	0.50	0.16	0.08	0.15	0.23	0.31	0.43	0.58	0.27
8-yr Average	0.87	0.58	0.20	0.10	0.12	0.19	0.29	0.44	0.74	0.28

Table 5. Fraction of the heating load supplied by system B

	Sep.	Oct.	Nov.	Dec.	Jan.	Feb.	Mar.	Apr.	May	Average
Calculated from the simulation										
1948–49	1.00	0.88	0.31	0.32	0.21	0.37	0.50	0.78	0.97	0.47
1949–50	0.99	0.97	0.40	0.26	0.7	0.32	0.44	0.58	0.88	0.45
1950–51	0.99	0.95	0.40	0.25	0.28	0.23	0.44	0.48	0.99	0.41
1951–52	0.97	0.75	0.36	0.17	0.19	0.35	0.48	0.66	0.87	0.42
1952–53	1.00	0.90	0.52	0.18	0.15	0.30	0.47	0.62	0.77	0.44
1953–54	1.00	0.90	0.54	0.22	0.23	0.42	0.54	0.74	0.77	0.49
1954–55	0.97	0.81	0.33	0.16	0.22	0.34	0.57	0.97	1.00	0.45
1955–56	1.00	0.79	0.30	0.17	0.27	0.40	0.55	0.72	0.71	0.44
8-yr average	0.99	0.87	0.39	0.22	0.23	0.34	0.50	0.69	0.87	0.45
Average year	0.97	0.79	0.35	0.26	0.23	0.36	0.53	0.72	0.77	0.45
Estimated from the performance chart										
1948–49	1.00	0.85	0.26	0.32	0.23	0.40	0.54	0.84	1.00	0.49
1949–50	1.00	0.98	0.40	0.25	0.28	0.35	0.49	0.61	1.00	0.47
1950–51	1.00	0.93	0.39	0.27	0.31	0.28	0.47	0.56	1.00	0.43
1951–52	1.00	0.73	0.37	0.18	0.21	0.37	0.53	0.77	0.98	0.45
1952–53	1.00	0.83	0.49	0.17	0.16	0.33	0.52	0.63	0.94	0.45
1953–54	1.00	0.99	0.50	0.21	0.25	0.43	0.55	0.80	0.94	0.51
1954–55	1.00	0.67	0.30	0.15	0.24	0.38	0.60	0.96	1.00	0.45
1955–56	1.00	0.81	0.31	0.18	0.29	0.43	0.57	0.74	0.89	0.47
8-yr average	1.00	0.85	0.38	0.21	0.25	0.37	0.53	0.74	0.97	0.47

Table 6. Fraction of the heating load supplied by system *C*

	Sep.	Oct.	Nov.	Dec.	Jan.	Feb.	Mar.	Apr.	May	Average
Calculated from the simulation										
1948–49	1.00	1.00	0.56	0.58	0.40	0.66	0.86	0.96	1.00	0.70
1949–50	1.00	1.00	0.67	0.49	0.49	0.58	0.77	0.87	0.96	0.68
1950–51	1.00	1.00	0.71	0.48	0.52	0.44	0.75	0.73	1.00	0.64
1951–52	1.00	0.99	0.67	0.34	0.36	0.64	0.79	0.90	0.99	0.65
1952–53	1.00	1.00	0.76	0.34	0.29	0.55	0.73	0.94	0.89	0.64
1953–54	1.00	1.00	0.79	0.42	0.43	0.72	0.87	0.90	0.98	0.71
1954–55	1.00	1.00	0.55	0.31	0.41	0.63	0.87	1.00	1.00	0.65
1955–56	1.00	0.98	0.58	0.33	0.52	0.71	0.92	0.93	0.90	0.69
8-yr average	1.00	1.00	0.66	0.41	0.43	0.62	0.82	0.90	0.96	0.67
Average year	1.00	0.98	0.63	0.49	0.43	0.66	0.85	0.96	0.88	0.69
Estimated from the performance chart										
1948–49	1.00	1.00	0.47	0.56	0.42	0.69	0.85	1.00	1.00	0.70
1949–50	1.00	1.00	0.67	0.45	0.51	0.62	0.78	0.91	1.00	0.69
1950–51	1.00	1.00	0.66	0.49	0.54	0.50	0.77	0.84	1.00	0.66
1951–52	1.00	0.98	0.63	0.34	0.39	0.64	0.83	1.00	1.00	0.66
1952–53	1.00	1.00	0.77	0.31	0.30	0.57	0.83	0.92	1.00	0.66
1953–54	1.00	1.00	0.79	0.39	0.45	0.71	0.86	1.00	1.00	0.72
1954–55	1.00	0.92	0.53	0.28	0.45	0.65	0.92	1.00	1.00	0.65
1955–56	1.00	1.00	0.54	0.34	0.53	0.72	0.89	1.00	1.00	0.70
8-yr average	1.00	0.99	0.63	0.40	0.45	0.64	0.84	0.96	1.00	0.68

Table 7. Fraction of the heating load supplied by system *D*

	Sep.	Oct.	Nov.	Dec.	Jan.	Feb.	Mar.	Apr.	May	Average
Calculated from the simulation										
1948–49	1.00	1.00	0.73	0.78	0.56	0.85	0.98	1.00	1.00	0.84
1949–50	1.00	1.00	0.81	0.70	0.65	0.77	0.92	0.99	0.99	0.83
1950–51	1.00	1.00	0.92	0.66	0.72	0.61	0.91	0.90	1.00	0.79
1951–52	1.00	1.00	0.87	0.49	0.52	0.84	0.94	0.99	1.00	0.79
1952–53	1.00	1.00	0.89	0.48	0.43	0.74	0.87	0.99	0.97	0.76
1953–54	1.00	1.00	0.90	0.59	0.60	0.89	0.97	0.98	1.00	0.83
1954–55	1.00	1.00	0.71	0.44	0.57	0.83	0.97	1.00	1.00	0.77
1955–56	1.00	1.00	0.80	0.48	0.72	0.89	1.00	1.00	0.99	0.82
8-year average	1.00	1.00	0.83	0.58	0.60	0.80	0.94	0.98	0.99	0.80
Average year	1.00	1.00	0.81	0.70	0.60	0.86	0.97	0.99	0.99	0.84
Estimated from the performance chart										
1948–49	1.00	1.00	0.61	0.72	0.56	0.86	0.99	1.00	1.00	0.82
1949–50	1.00	1.00	0.82	0.60	0.66	0.79	0.94	1.00	1.00	0.82
1950–51	1.00	1.00	0.81	0.64	0.70	0.66	0.92	0.97	1.00	0.79
1951–52	1.00	1.00	0.79	0.47	0.54	0.81	0.99	1.00	1.00	0.78
1952–53	1.00	1.00	0.91	0.43	0.43	0.74	0.97	1.00	1.00	0.77
1953–54	1.00	1.00	0.92	0.53	0.60	0.87	1.00	1.00	1.00	0.83
195455	1.00	1.00	0.67	0.40	0.60	0.82	1.00	1.00	1.00	0.76
1955–56	1.00	1.00	0.70	0.47	0.69	0.89	1.00	1.00	1.00	0.81
8-yr average	1.00	1.00	0.78	0.53	0.60	0.80	0.98	1.00	1.00	0.80

the heating load is small relative to the yearly total heating load. For the 9-month period, the differences are reasonably small for all four systems. This result suggests that the weather sequences occurring in the "average" year, chosen in the manner described previously, are representative to those occurring in the long term. The use of an average year defined in this manner is recommended for use in simulations intended to provide an estimate of long-term system performance. The inaccuracies introduced in the predictions of long-term system performance are believed to be small in comparison with those attributed to simplifications in the simulation model, uncertainties in the recorded radiation data, and to the prediction of future weather conditions. The "average" year for Madison has been used to obtain most of the information for the design procedure described in Part III.

PART III. A DESIGN PROCEDURE FOR SOLAR HEATING SYSTEMS

III.1 *The approach*

One approach to the problem of determining an economic solar heating system design is to use the simulation model described in Part I directly as a design tool. But the use of computer simulations to aid in the design of every solar heated building is, in general, unsatisfactory, particularly for those architects and

heating engineers concerned with the design of small buildings who do not have access to computing facilities.

Recognizing the need for a simple means of estimating the long-term performance of solar heating systems, Hottel and Whillier[2] developed the concept of "utilizability" and the ϕ-curves. The ϕ-curves are a set of performance curves dependent only upon location from which the monthly thermal performance of a collector of any size and construction can easily be estimated. The ϕ-curves were later extended by Liu and Jordan[5] into the generalized ϕ-curves which are location independent as well. The basic problem with the ϕ-curves is that they require a specification of the average critical radiation intensity which, in most cases, is indeterminate.

The approach adopted here has been to use simulations to develop a generalized performance chart involving less restrictive assumptions than those required by the ϕ-curves. The performance chart correlates the long-term performance of solar heating systems to the system design parameters, the building construction, and the weather. Combined with costs in the location in question, this chart provides a method by which architects and heating engineers can determine the economic optimum design of residential solar space and water heating systems using liquid heat transport.

III.2 *Sensitivity analysis*

The development of a general design procedure for solar heating systems begins with an extensive study of the effects of the design parameters upon the long-term system performance. Several design parameters have been found to have only a small effect upon system performance for a wide range of values of practical interest. These results, in general agreement with the conclusions of others, are summarized as follows.

Collector fluid capacitance rate

The optimum collector fluid capacitance rate, i.e. the rate at which energy collection is maximized, is infinitely large. However, the dependence of system performance on the collector capacitance rate is asymptotic; as shown in Duffie and Beckman[4] only a small gain in energy collection is realized if the collector fluid capacitance rate (per unit collector area) is increased when the collector flow factor, defined in eqn (16), exceeds about 0.95.

$$F'' = F_R/F' = \frac{(\dot{m}C_p)_c}{AU_LF'}\left[1 - \exp\left(\frac{-U_LF'A}{(\dot{m}C_p)_c}\right)\right]. \quad (16)$$

Low collector capacitance rates, e.g. rates for which $(\dot{m}C_p)_c/AU_LF'$ is less than about 5, can reduce energy collection significantly particularly if the fluid boils and energy must be "dumped" through the pressure relief valve. All following results have been obtained using a collector capacitance rate of 210 kJ hr^{-1} C^{-1} m^{-2}, although the correlations developed in the next section are applicable to all capacitance rates in this general range.

Storage capacity

In their economic study of solar house heating, Lof and Tybout[18] concluded that the storage tank capacity resulting in minimum cost solar heat is in the range of 200–300 kJ C^{-1} (50–75 kg of stored water) per square meter of collector area. In addition, they indicated that the performance of solar heating systems is rather insensitive to the amount of storage capacity within this general range. The results of simulations for several storage capacities in the Madison climate are in general agreement with Lof and Tybout as shown in Fig. 2. A storage capacity of 75 kg H_2O m^{-2} has been used to obtain all following results.

Load heat exchanger size

The dimensionless parameter $\epsilon_L C_{min}/UA$ has been found to provide a measure of the size heat exchanger needed to supply solar heat to a specified building. The graph in Fig. 3 shows how the performance of a space heating system (expressed as the ratio of the load fraction supplied by solar to that which would have been supplied if an infinitely large heat exchanger were used) is related to $\epsilon_L C_{min}/UA$. For values of $\epsilon_L C_{min}/UA$ less than 1, the reduction in system performance due to too small a heat exchanger will be appreciable. Reasonable values of $\epsilon_L C_{min}/UA$ for solar space heating systems are between 1 and 3 when costs are considered. All following results have been obtained with $\epsilon_L C_{min}/UA$ equal to 2.

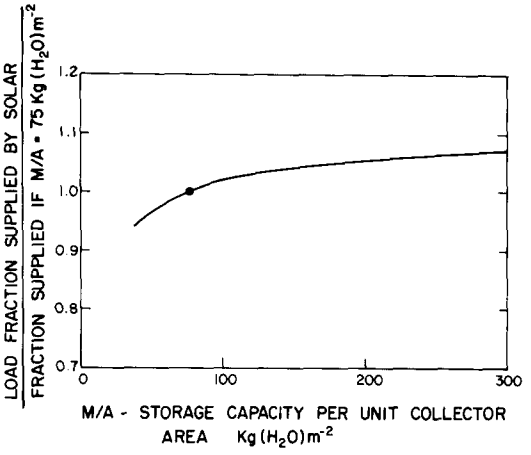

Fig. 2. Effect of storage capacity.

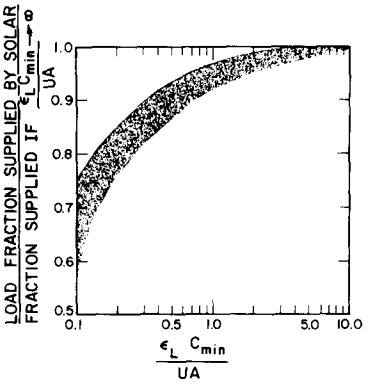

Fig. 3. Effect of load heat exchanger size.

III.3 *Correlation of system performance*

The performance of solar heating systems is sensitive to the design parameters ($F'_R A$), U_L, ($\tau\alpha$), s, and to the parameters influencing the total space and water heating loads. The economic optimum values of these parameters depend upon the weather and the costs in the location in question.

The results presented in Part II demonstrated that it is possible to use an "average" year of meteorological data in a simulation to provide an estimate of solar heating system performance for the long term. The "average" year, chosen only on the criterion that the total insolation and degree hours for each month be approximately equal to the 8-year average, undoubtedly has weather sequences differing from those occurring in the 8-year period. However, a reasonable estimate of the 8-year average performance of all four systems examined was possible with the "average" year of data. This fact suggests that the system performance for a specified period may be correlated to the total insolation and heating load during the period, and to the parameters characterizing the system design. The appropriate parameters can be identified by integrating eqn (10) with respect to time for a period Δt

$$MC_v \int^{\Delta t} \frac{dT}{dt}\,dt = \int^{\Delta t} Q_d\,dt - \int^{\Delta t} (Q_L + Q_w)\,dt + \int^{\Delta t} (E_L + E_w)\,dt. \quad (17)$$

The integration period Δt can be chosen to be sufficiently long so that the term on the left hand side of eqn (17) becomes small in respect to the other terms. For the storage sizes considered, a one month integration period is sufficient. An expression for Q_d is given in eqn (8). The time integral of $(Q_L + Q_w)$ is the total heating load L during the integration period.

$$L = \int^{\Delta t} (Q_L + Q_w)\,dt. \quad (18)$$

The last term of eqn (17) represents the total auxiliary energy E required in addition to the energy supplied by solar energy in order to satisfy the heating load during the integration period.

$$E = \int^{\Delta t} [E_L + E_w]\,dt \quad (19)$$

eqn (17) can thus be expressed†

$$f = \frac{L - E}{L} = \frac{F'_R A}{L} \int^{\Delta t} [H_T(\tau\alpha) - U_L(T - T_a)]^+\,dt \quad (20)$$

†Equation (20) assumes that $T_1 \le T_{max}$.

‡The information in Fig. 4 can be described by the relation

$$f = 1.029Y - 0.065Z - 0.245Y^2 + 0.0018Z^2 + 0.0215Y^3$$

where $Y = F'_R AS(\overline{\tau\alpha})/L$ and $Z = F'_R AU_L(T_{ref} - \bar{T}_a)\Delta t/L$.

where f is the fraction of the total heating load which is supplied by solar energy.

It is convenient to multiply and divide the last term of eqn (20) by $(T_{ref} - T_a)$ where T_{ref} is a reference temperature chosen to be 100°C. Then f can be expressed in terms of a dimensionless inlet temperature X.

$$f = \frac{F'_R A}{L} \int^{\Delta t} [H_T(\tau\alpha) - U_L(T_{ref} - T_a)X]^+\,dt \quad (21)$$

where

$$X = \frac{(T - T_a)}{(T_{ref} - T_a)}. \quad (22)$$

Equation (21) cannot be used to calculate f directly, since X is a complicated function of L, H_T and T_a, and the integral cannot be explicitly evaluated. However, eqn (21) suggests that f may be empirically related to the two dimensionless groups in eqns (23) and (24).

$$\frac{F'_R A}{L} \int^{\Delta t} H_T(\tau\alpha)\,dt = \frac{F'_R A}{L} S(\overline{\tau\alpha}) \quad (23)$$

$$\frac{F'_R A}{L} \int^{\Delta t} U_L(T_{ref} - T_a)\,dt = \frac{F'_R A}{L} U_L(T_{ref} - \bar{T}_a)\Delta t. \quad (24)$$

These dimensionless groups have some physical significance. $F'_R AS(\tau\alpha)/L$ is the ratio of the total energy absorbed on the collector plate surface to the total heating load during the period Δt. $F'_R AU_L(T_{ref} - \bar{T}_a)\Delta t/L$ is the ratio of a reference collector plate energy loss (for water based systems) to the total heating load during the period Δt.

The obvious choice for Δt is 1 month (in appropriate units). Monthly average ambient temperatures can be found in Ref. [27]. The monthly total (space and water) heating load L can be estimated from the daily average degree-days tabulated in ASHRAE[26] or in Ref. [27] for each month for many locations in U.S. A method of estimating S, the monthly total radiation on a tilted collector surface, from records of the average daily radiation on a horizontal surface is given in Appendix 1.

The correlation of f to $F'_R AS(\overline{\tau\alpha})/L$ and $F'_R AU_L(T_{ref} - \bar{T}_a)\Delta t/L$ has been investigated using the simulation model described in Part I. Each simulation estimated month by month system performance by performing calculations at half-hourly intervals using meteorological data for the average Madison year. The results of over 300 simulations for which the design parameters were varied in the ranges indicated in Table 8 have shown that f is well correlated to $F'_R AS(\overline{\tau\alpha})/L$ and $F'_R AU_L(T_{ref} - \bar{T}_a)\Delta t/L$ in the manner shown in Fig. 4.‡ Figure 4 allows the performance of a

Table 8. Range of values of the design parameters examined

0.6	≤ $(\tau\alpha)_n$ ≤	0.9	dimensionless	
5.0	≤ $(F'_R A)$ ≤	120.0	m^2	
7.5	≤ U_L ≤	30.0	kJ hr^{-1} C^{-1} m^{-2}	
30	≤ s ≤	90	degrees	
300.0	≤ UA ≤	2400	kJ hr^{-1} C^{-1}	
140	≤ D ≤	560	kg day^{-1}	

solar heating system to be simply estimated, month by month, as a function of the system design and the local weather. Since the chart has been generated empirically, its merit cannot be proven, but only demonstrated. Tables 4–7 compare the values of f, determined by simulation, with values estimated directly from Fig. 4 for systems A, B, C and D (see Table 3) at month by month intervals for the 8-year period in Madison.

performance chart estimations were found to compare surprisingly well with the simulation results. The standard errors of the differences between the simulated and estimated yearly average values of f for the four locations were in fact as small or smaller than the standard error of 0.015 incurred for the 8-years of Madison data.

One explanation of the excellent agreement between the simulation results and the performance chart estima-

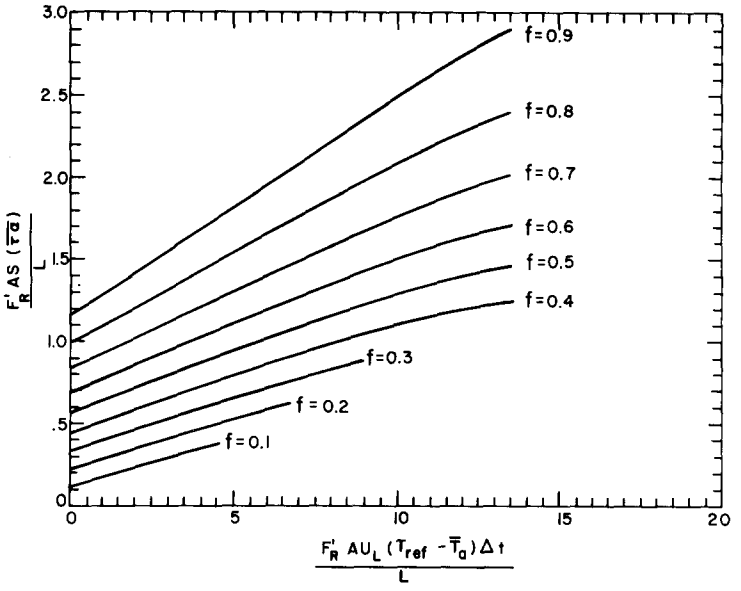

Fig. 4. Performance chart for solar heating systems.

Although significant differences between the simulated and estimated values of f for monthly periods can be found (generally for months in which the heating load is small relative to the yearly total heating load), the correlation appears to be quite satisfactory in most cases. It should be emphasized, however, that Fig. 4 is not intended to provide an accurate estimate of system performance for any particular month, but rather for the year average or the long-term. The differences between the simulated and estimated yearly average values of f, in Tables 4–7, are small. The standard error of the differences is 0.015, an error judged to be substantially lower than the errors inherent in the simulation model and the recorded data.

III.4 *Location independence*

Figure 4 has been developed using simulation results for the Madison "average" year. However, it has been demonstrated in Tables 4–7 that it can be used more generally to estimate solar heating system performance for other years of Madison meteorological data. It has been found that the performance chart can be applied for other locations with satisfactory results.

The simulated performance of systems in Blue Hill, Mass., Charleston, South Carolina, Albuquerque, New Mexico and Boulder, Colorado have been compared with the performances estimated from Fig. 4. Four systems designs, chosen to provide from 25 to 90 per cent of the heating load, were examined in each location. The tions can be found in the method used in the simulation model to estimate radiation data on a tilted surface from measurements on a horizontal surface. As discussed in Part I, the actual fluctuations of the radiation intensity during the day, which will typically differ in each location, cannot be represented using the method described. However, the actual distribution of the radiation intensity during each day has only a small effect on the long-term system performance. In any case, the estimate provided by the performance chart will always be conservative in this respect.

III.5 *Comparison with experimental results*

Many solar heated buildings have been constructed[23]; unfortunately, in only a few of these installations has detailed system performance data been measured and reported for extended periods.

Engebretson[24] has reported the monthly performance of M.I.T. Solar House IV for two heating seasons in Blue Hill, Mass. The heating system used in Solar House IV is similar to that shown in Fig. 1. The major difference is that the Solar House IV collectors were gravity-drained when not in operation and the system did not include a separate collector flow loop and heat exchanger as in Fig. 1. The important design parameters of the Solar House IV system are listed in Table 9. A comparison of the experimental performance of Solar House IV with the performance estimated from the performance chart (Fig. 4), is given in Table 10.

Table 9. Design parameters of Solar House IV [24]

A	59.5	m^2
$(\dot{m}C_p)_c$	10170.0	kJ hr^{-1} C^{-1}
U_L	14.3	kJ hr^{-1} C^{-1} m^{-2}
F'_R	0.86	
$(\overline{\tau\alpha})$	0.70	
s	60	degrees
M/A	108.1	kg H_2O m^{-2}
UA	950	kJ hr^{-1} C^{-1}
C_{min}	1738	kJ hr^{-1} C^{-1} (air)
ϵ_I	0.78	
$\epsilon_I C_{min}/UA$	1.42	
T_R	21.6	C

and water heating requirements of a three bedroom residence in Madison, Wisconsin (latitude 43°N). The space heating load is characterized by a UA value of 1360 kJ hr^{-1} $°C^{-1}$. The water heating load is estimated to be 300 l per day, heated from the mains supply temperature, 11°C, to at least 60°C. Single-glazed collectors, tested by the method of Vernon and Simon [25], are to be used. The necessary design characteristics of these collectors, $F_R U_L = 17.6$ kJ hr^{-1} $°C^{-1}$ m^{-2} and $F_R(\tau\alpha)_n = 0.77$ are determined from the slope and intercept of the NASA–Lewis performance curves. $(\overline{\tau\alpha})$ is approximately 0.93 per cent of $(\tau\alpha)_n$ and so $F_R(\overline{\tau\alpha}) = 0.72$. F'_R/F_R, determined from eqn (6) with $(\dot{m}C_p)_c/A = 210$ kJ $°C^{-1}$ hr^{-1} m^{-2} and $\epsilon_C = 0.7$, is 0.97. The collectors are to be mounted facing due south at a slope equal to the latitude. The ratio of the storage tank capacity to collector area is to be 75 kg (H_2O) m^{-2}. (The effect of a change in storage capacity can be estimated from Fig. 2.)

Table 10. Comparison with the experimental results of Solar House IV fraction of the heating load supplied by solar energy

	Oct.	Nov.	Dec.	Jan.	Feb.	Mar.	Apr.	Year average
				Reported by Engebretson [24]				
1959–60	0.97	0.25	0.30	0.38	0.51	0.61	0.67	0.48
1960–61	0.98	0.74	0.45	0.44	0.59	0.60		0.57
				Estimated from Fig. 4				
1959–60	0.96	0.40	0.39	0.49	0.56	0.66	0.76	0.56
1960–61	0.98	0.72	0.53	0.50	0.63	0.70		0.62

The load fractions estimated from Fig. 4 are somewhat higher than the values reported by Engebretson; the yearly average value is 8 per cent higher for the 1959–60 heating season and 5 per cent higher for 1960–61. These differences, however, are not necessarily due to inadequacies of the performance chart or the simulation model. They could be due to difficulties in operation of Solar House IV during its first years of operation. It is interesting to note that, in comparing the experimental performance with the theoretical performance estimated by the ϕ-curve method, Engebretson concluded that "... Solar House IV could utilize from four to ten percent more of the available radiation than it does".

III.6 *Use of the performance chart*

In this section, an example is given showing how the performance chart can be used to select an economically optimal solar heating system. The problem is to determine the best collector size to provide a portion of the space and water heating requirements of a three bedroom residence in Madison, Wisconsin (latitude 43°N). The average solar radiation S incident on a 43° surface in Madison for each calendar month is estimated in Appendix 1. The average monthly heating load L is the sum of the space and water heating loads. The space heating load for each month is the product of UA and the average °C-hr for each month, tabulated (in units of °F-days) in ASHRAE [26] or in the annual summary of local climatological data available from NOAA [27]. Monthly average ambient temperatures are also available in the latter reference. This information for Madison is given in Table 11.

The fraction of the heating load supplied by solar energy during each month for each collector size

Table 11. Average meteorological information for Madison, Wisconsin

Month	S (kJ $m^{-2} \times 10^{-6}$)	Heating (°C-hr)	$\bar{T}_a$ (°C)	Space heating load (kJ $\times 10^{-6}$)	Water heating load (kJ $\times 10^{-6}$)	L, Total heating load (kJ $\times 10^{-6}$)
Jan.	0.382	19640	−8.1	26.71	1.91	28.62
Feb.	0.405	16990	−6.0	23.11	1.72	24.83
Mar.	0.557	14840	−0.2	20.18	1.91	22.09
Apr.	0.512	8240	7.9	11.21	1.85	13.06
May	0.555	4130	13.8	5.62	1.91	7.53
June	0.588	1360	19.4	1.85	1.85	3.70
July	0.620	330	21.8	0.45	1.91	2.36
Aug.	0.600	530	20.9	0.72	1.91	2.63
Sept.	0.584	2320	16.0	3.16	1.85	5.01
Oct.	0.522	6320	10.5	8.60	1.91	10.51
Nov.	0.330	12400	1.9	16.86	1.85	18.71
Dec.	0.357	17730	−5.2	24.11	1.91	26.02

considered† can be determined from the performance chart as a function of the dimensionless parameters $F'_R AS(\overline{\tau\alpha})/L$ and $F'_R AU_L(T_{ref} - \bar{T}_a)\Delta t/L$. The estimated system performance for collectors of 20, 40, 80 and 120 m^2 is given in Table 12. The yearly average load fractions supplied by these collectors are plotted against collector area in Fig. 5.

Combined with a knowledge of costs, the information in Fig. 5 can be used to determine the economic optimum collector size. For example, assume that the collectors are available at an installed cost of \$80/m^2 plus a fixed cost of \$500 for additional equipment such as the heat exchanger, pumps, pump controller and piping. Insulated steel water storage tanks cost approximately \$0.18/kg for the range of sizes considered. An annual charge of 12 per cent is assumed on the capital investment. The yearly dollar savings in using solar heating can then be expressed as a function of collector area, and auxiliary fuel cost C_F.

†A simple method of using Fig. 4 when estimating the performance of more than one collector size is to construct a straight line through the origin and a point corresponding to a known collector area, for example 100 m^2. Along this line, the meteorological conditions for the month and all design parameters except collector area are fixed. The line is the collector area axis, and it can be scaled to facilitate a crossplot of load fraction vs collector area for each month.

Dollar savings =

$$C_F \sum_1^{12} fL - 0.12\left[[80 + (0.18)(75)]A + 500\right]. \tag{25}$$

Dollar Savings has been plotted vs collector area for several values of fuel costs in Fig. 6. For the costs assumed in this example, it can be seen in Fig. 6 that fuel costs must be about \$6/10^6 kJ before a dollar savings using solar heating can occur.

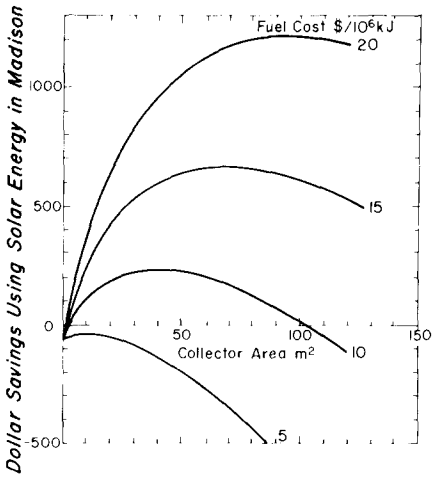

Fig. 6. Dollar savings using solar heating in Madison.

Table 12. Estimated solar heating system performance: Madison, Wisconsin

Month	$F'_R S(\overline{\tau\alpha})/L$ (m^{-2})	$F'_R U_L(T_{ref} - T_a)\Delta t/L$ (m^{-2})	f—fraction of LOAD supplied by Solar A = 20 m^2	A = 40 m^2	A = 80 m^2	A = 120 m^2
Jan.	0.0093	0.0477	0.11	0.23	0.42	0.56
Feb.	0.0114	0.0487	0.15	0.30	0.53	0.69
Mar.	0.0175	0.0573	0.25	0.47	0.76	0.91
Apr.	0.0274	0.0862	0.39	0.67	0.94	1.0
May	0.0515	0.1446	0.67	0.96	1.0	1.0
June	0.1110	0.3651	0.95	1.0	1.0	1.0
July	0.1835	0.4188	1.0	1.0	1.0	1.0
Aug.	0.1593	0.3801	1.0	1.0	1.0	1.0
Sept.	0.0839	0.2050	0.88	1.0	1.0	1.0
Oct.	0.0347	0.1076	0.47	0.77	1.0	1.0
Nov.	0.0123	0.0641	0.15	0.29	0.51	0.66
Dec.	0.0096	0.0511	0.11	0.23	0.42	0.57
Year average			0.28	0.44	0.65	0.76

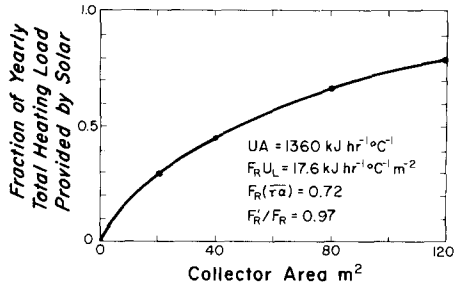

Fig. 5. Fraction of heating load supplied by solar energy in Madison.

Figure 6 also shows that the dollar savings using solar heating is not a strong function of collector area in a large range about the optimum. An error as large as 10 or 15 m^2 in the estimate of the optimum collector size generally has little effect upon the cost of solar heating. Thus, small errors in the estimate of the long-term thermal performance of solar heating systems should be of no major concern.

NOMENCLATURE

A collector area, m^2
C_F cost of auxiliary fuel, $ per 10^6 kJ of energy delivered
C_{min} minimum capacitance rate in the load heat exchanger, kJ hr^{-1} $°C^{-1}$
C_p fluid specific heat, kJ kg^{-1} $°C^{-1}$
D average daily hot water demand, kg day^{-1}
E integrated total auxiliary energy required during the period Δt, kJ
E_l rate at which auxiliary energy supplements the space heating load, kJ hr^{-1}
E_w rate at which auxiliary energy supplements the water heating load, kJ hr^{-1}
f fraction of the heating load supplied by solar energy
F' collector efficiency factor
F'' collector flow factor defined in eqn (16)
F_R collector heat removal factor defined in eqn (2)
F'_R collector-heat exchanger efficiency factor defined in eqn (7)
H radiation incident on a horizontal surface, kJ m^{-2} hr^{-1}
H_b rate of beam radiation incident on a horizontal surface, kJ hr^{-1} m^{-2}
H_d rate of diffuse radiation incident on a horizontal surface, kJ hr^{-1} m^{-2}
H_T rate of total radiation incident on the (tilted) collector surface, kJ hr^{-1} m^{-2}
$\bar{H}$ monthly average of the daily radiation incident on a horizontal surface, kJ m^{-2} day^{-1}
$\bar{H}_0$ monthly average of the daily extraterrestrial radiation, kJ m^{-2} day^{-1}
K_T ratio of the daily total radiation on a horizontal surface to the extraterrestrial radiation
$\bar{K}_T$ ratio of the monthly averages of the daily radiation on a horizontal surface to the extraterrestrial radiation
L integrated total (space and water) heating load during the period Δt, kJ
$(mC_p)_c$ collector fluid capacitance rate, kJ $°C^{-1}$ hr^{-1}
$(\dot{m}C_p)_{min}$ minimum of $(mC_p)_c$ and $(mC_p)_s$
$(mC_p)_s$ fluid capacitance rate in the flow circuit between the tank and the collector heat exchanger, kJ$°C^{-1}$ hr^{-1}
$(mC_p)_w$ capacitance rate of the water extracted from the tank to supply the water heating load, kJ$°C^{-1}$ hr^{-1}
M mass of water in the storage tank, kg H_2O
Q_d rate at which collected energy is delivered to the tank, kJ hr^{-1}
Q_{hx} rate at which energy is transferred in the collector-tank heat exchanger, kJ hr^{-1}
Q_L space heating load, kJ hr^{-1}
Q_{max} maximum rate at which energy can be transferred in the space heating load heat exchanger, kJ hr^{-1}
Q_u Rate of energy collection by the flat-plate collector, kJ hr^{-1}
Q_w water heating load, kJ hr^{-1}
R_b ratio of the direct radiation incident on a tilted surface to that on a horizontal surface
$\bar{R}$ ratio of the monthly average of daily radiation on a tilted surface to that on a horizontal surface (tabulated in Appendix 1)
s slope of the collector, degrees
S total radiation incident on the collector surface during the period Δt, kJ
t time, hours
T storage tank temperature, °C
T_a ambient temperature, °C
T_{env} temperature to which storage tank energy losses occur, °C
T_i temperature of the fluid at the collector inlet, °C
T_m temperature of mains supply water, °C
T_{max} boiling temperature, °C
T_0 temperature of the fluid at the collector outlet, °C
T_r indoor temperature reduced to account for internal energy generation, 18.3°C
T_{ref} reference temperature, 100°C
T_R indoor temperature, 20°C
T_w minimum acceptable temperature for hot water, °C
T_1 temperature of the fluid entering the relief valve, °C
UA constant characterizing the space heating load, kJ hr^{-1} $°C^{-1}$
$(UA)_s$ coefficient of energy losses from the tank, kJ hr^{-1} $°C^{-1}$
U_L collector overall energy loss coefficient, kJ hr^{-1} $°C^{-1}$ m^{-2}
X dimensionless temperature defined in eqn (22)
δ solar declination, degrees
Δt one month time period, hours
ϕ latitude, degrees
ϵ_c effectiveness of the collector-tank heat exchanger
ϵ_L effectiveness of the space heating load heat exchanger
ρ ground reflectance
$(\tau\alpha)$ product of the cover transmittance and the plate absorptance accounting for dirt and shading
$(\tau\alpha)_n$ $(\tau\alpha)$ at normal radiation incidence
$(\overline{\tau\alpha})$ weighted monthly average value of $(\tau\alpha).(\overline{\tau\alpha})/(\tau\alpha)$ is approximately 0.93 and 0.91 for 1 and 2 glass flat-black absorbers tilted from 0° to 15° greater than the latitude
ω hour angle, degrees
ω_s sunset hour angle, degrees

REFERENCES

1. TRNSYS, A transient simulation problem, Engineering Experiment Station Report No. 38. Solar Energy Laboratory, University of Wisconsin, Madison, Wisconsin.
2. H. C. Hottel and A. Whillier, Evaluation of flat-plate solar collector performance. *Trans. of the Conference on the Use of Solar Energy*, **II**. Thermal Processes, 74–104. University of Arizona, Tempe, Arizona (1955).
3. S. A. Klein, J. A. Duffie and W. A. Beckman, Transient considerations of flat-plate solar collectors. *ASME Journal of Engineering for Power* **96**(2) (1974).
4. J. A. Duffie and W. A. Beckman, *Solar Energy Thermal Processes*. Wiley, New York (1974).
5. B. Y. H. Liu and R. C. Jordan, The long-term average performance of flat-plate solar energy collectors. *Solar Energy* **7**(2), 53 (1963).
6. B. Y. H. Liu and R. C. Jordan, The interrelationship and characteristic distribution of direct, diffuse and total solar radiation. *Solar Energy* **4**(3) (1960).
7. D. J. Close, A design approach for solar processes. *Solar Energy* **11**, 112–122 (1967).
8. A. Whillier, Solar energy collection, and its utilization for house heating. *Sc.D. Thesis*, M.I.T. Cambridge, Mass. (1953).
9. R. W. Bliss, The derivation of several 'plate-efficiency factors' useful in the design of flat-plate solar heat collectors. *Solar Energy* **3**(4), 55–64 (1959).
10. S. A. Klein, Calculation of flat-plate collector loss coefficients. *Solar Energy* **17**, 79–80 (1975).
11. W. M. Kays and A. L. London, *Compact Heat Exchangers*. McGraw-Hill, New York (1958).
12. F. de Winter, Heat exchanger penalties in double loop solar water heating systems. *Solar Energy* **17**, 335–338 (1976).
13. G. Gutierrez, *et al.*, Simulation of forced circulation water heaters; effects of auxiliary energy supply, load type, and storage capacity. *Solar Energy* **15**, 287–298 (1974).
14. M. Lokmanhekim, Ed., *Procedure for Determining Heating and Cooling Loads for Computerized Energy Calculations*. ASHRAE, New York (1971).
15. R. A. Grot, Energy utilization in a residential community. NSF-RANN Grant GI-34994, Princeton University, Session IV, Proceedings of the *Solar Heating and Cooling for Buildings Workshop*, Part I: Technical Sessions, 21,22 March 1973. Prepared for National Science Foundation by the Dept. of Mechanical Engineering, Univ. of Maryland.
16. *Handbook of Fundamentals*, Chap. 20. ASHRAE, New York, N.Y. (1972).
17. J. J. Mutch, Residential water heating: fuel consumption, economics and public policy. RAND, Dept. R 1498, National Science Foundation (May 1974).
18. G. O. G. Lof and R. A. Tybout, Cost of house heating with solar energy. *Solar Energy* **19**, 253–278 (1973).

19. H. Buchberg and J. R. Roulet, Simulation and optimization of solar collection and storage for house heatings. *Solar Energy* **12**(1), 1–50 (1968).
20. L. W. Butz, W. A. Beckman and J. A. Duffie, Simulation of a solar heating and cooling system. *Solar Energy* **16**, 129–136 (1974).
21. R. L. Oonk, W. A. Beckman and J. A. Duffie, Modeling of the CSU heating/cooling system. *Solar Energy* **17**, 21–28 (1975).
22. R. F. Benseman and F. W. Cook, Solar radiation in New Zealand—the 'standard year'. *N.Z. Journal of Science* **12**, 698–708 (1969).
23. G. O. G. Lof, Use of solar energy for heating purposes: space heating. *Proc. of the UN Conf. on New Sources of Energy*, Vol. 5, UN, New York, pp. 114–124 (1964).
24. C. D. Engebretson, The use of solar energy for space heating: MIT Solar House IV. *Proc. of the UN Conf. on New Sources of Energy* **5**, 159. United Nations, New York, N.Y. (1964).
25. R. W. Vernon and F. F. Simon, Flat-plate collector performance determined experimentally with a solar simulator. Paper presented at Ft. Collins ISES meeting, August 1974 and NASA TMX-71602.
26. ASHRAE, 1973 Systems, Chapter 43.
27. Annual Summary of Local Climatological Data, National Oceanic and Atmospheric Administration, Environmental Data Service, National Climatic Center, Asheville, N.C.
28. B. Y. H. Liu and R. C. Jordan, Availability of solar energy for flat-plate solar heat collectors, in *Low Temperature Engineering Applications of Solar Energy*. ASHRAE, New York, N.Y. (1967).
29. B. Y. H. Liu and R. C. Jordan, Daily insolation on surfaces tilted toward the equator. *Trans. ASHRAE*, 526–541 (1962).

APPENDIX 1

Calculation of radiation on tilted surfaces

Average daily totals of the radiation incident on a horizontal surface for each calendar month are available for many locations in the United States[28]. However, radiation data on tilted surfaces are generally not available. A simple method of estimating the average daily radiation for each calendar month on surfaces tilted directly towards the equator has been proposed by Lui and Jordan[29] and is presented here.

The average daily radiation on a horizontal surface, $\bar{H}$, for each calendar month can be expressed in terms of $\bar{K}_T$, the fraction of the mean daily extraterrestrial radiation, $\bar{H}_0$.

$$\bar{K}_T = \bar{H}/\bar{H}_0 \tag{1}$$

$$\bar{H}_0 = \frac{1}{\Delta t}\int^{\Delta t}\frac{24}{\pi}I_{sc}\left(1+0.033\cos\left(\frac{360n}{365}\right)\right)$$

$$\times[\cos\phi\cos\delta\sin\omega_s + \omega_s 2\pi/360\sin\phi\sin\delta]\,dt \tag{2}$$

where Δt is a one-month period; $\bar{H}_0$ for each month is tabulated as a function of latitude in Table A1.†

The average daily radiation on a tilted surface, $\bar{H}_T$, can be expressed

$$\bar{H}_T = \bar{R}\bar{H} = \bar{R}\bar{K}_T\bar{H}_0 \tag{3}$$

where $\bar{R}$ is defined to be the ratio of the daily average radiation on a tilted surface to that on a horizontal surface for each month. Liu and Jordan[29] have proposed that $\bar{R}$ can be expressed

$$\bar{R} = \left(1-\frac{\bar{D}}{\bar{H}}\right)R_D + \frac{\bar{D}}{\bar{H}}\left(\frac{1+\cos s}{2}\right) + \rho\left(\frac{1-\cos s}{2}\right) \tag{4}$$

where $\bar{D}$ is the average daily diffuse radiation for each month; s is the tilt of the surface; ρ is the ground reflectance; R_D is the ratio of the average daily beam radiation on the tilted surface to that on a horizontal surface for each month.

R_D is a function of the transmittance of the atmosphere, which in general varies in some unknown manner. However, Liu and Jordan suggest that R_D can be approximated by the ratio of the mean daily extraterrestrial radiation on a tilted surface to that on a

†Note that a more recent value of the solar constant than that used by Liu and Jordan[28] is available[4]. As a result, their values of $\bar{K}_T$ will differ slightly from those in Table A2.

Table A1. Monthly average daily extraterrestrial radiation, kJ m^{-2}

Latitude	Jan.	Feb.	Mar.	Apr.	May	June	July	Aug.	Sep.	Oct.	Nov.	Dec.
20	26644	30359	34307	37515	38884	39144	38893	37864	35300	31402	27512	25519
25	23902	28115	32848	37111	39356	40046	39606	37832	34238	29413	24909	22669
30	21034	25679	31141	36436	39569	40706	40071	37534	32917	27213	22161	19714
35	18069	23072	29200	35498	39530	41129	40292	36976	31348	24820	19296	16687
40	15043	20319	27040	34303	39247	41328	40281	36166	29542	22255	16344	13626
45	11998	17443	24677	32869	38737	41322	40055	35118	27515	19541	13344	10579
50	8987	14490	22131	31209	38025	41147	39644	33851	25283	16705	10342	7605
55	6082	11486	19423	29345	37152	40863	39100	32391	22863	13778	7396	4791
60	3395	8486	16576	27308	36188	40585	38513	30779	20277	10798	4598	2277

Table A2. Average radiation data for Madison, Wisconsin

Month	$\bar{H}$ (kJ m^{-2} day^{-1})	$\bar{H}_0$ (kJ m^{-2} day^{-1})	$\bar{K}_T$	$\bar{R}$	H_T (kJ m^{-2} day^{-1})	S (kJ m^{-2} mo.$^{-1}$ × 10^{-6})
Jan.	6412	13217	0.485	1.92	12311	0.382
Feb.	9224	18595	0.496	1.57	14469	0.405
Mar.	13992	25620	0.546	1.28	17977	0.557
Apr.	16527	33442	0.494	1.03	17059	0.512
May	19821	38942	0.509	0.90	17905	0.555
June	23073	41322	0.558	0.85	19606	0.588
July	23241	40145	0.578	0.86	20010	0.620
Aug.	19762	35538	0.556	0.98	19347	0.600
Sept.	16397	28327	0.579	1.19	19473	0.584
Oct.	11277	20629	0.547	1.49	16826	0.522
Nov.	6311	14544	0.434	1.74	10996	0.330
Dec.	5632	11720	0.480	2.05	11519	0.357

horizontal surface for the month. Using this approximation,

$$R_D \simeq \frac{\cos(\phi - s)\cos\delta \sin\omega_s' + \omega_s' \sin(\phi - s)\sin\delta}{\cos(\phi)\cos\delta\sin\omega_s + \omega_s \sin\phi \sin\delta} \quad (5)$$

where

$$\omega_s' = \min[\arccos(-\tan\phi\tan\delta), \arccos(-\tan(\phi - s)\tan\delta)].$$
$$\omega_s = \arccos(-\tan\phi\tan\delta) \quad (6)$$

Figure 8 in Ref. [29] provides a relationship between $\bar{D}/\bar{H}$ and $\bar{K}_T$. An empirical curve fit to the data in this figure yields

$$\frac{\bar{D}}{\bar{H}} = 1.3903 - 4.0273\bar{K}_T + 5.5315\bar{K}_T^2 - 3.108\bar{K}_T^3. \quad (7)$$

An example demonstrating the use of these relations follows.

Example

Estimate the average monthly total radiation incident on a 43° tilted surface in Madison, Wisconsin (43°N latitude).

Daily average values of $\bar{H}$ for each month can be found in Ref. [28]. The mean daily extraterrestrial radiation, $\bar{H}_o$, for each month is found in Table A1. The ratio $\bar{H}/\bar{H}_o$ determines $\bar{K}_T$ for each month which can then be used to calculate $\bar{D}/\bar{H}$ from eqn (7). $\bar{R}$ is calculated for each month from equations(4–6). The average daily radiation on a 43° surface, $\bar{H}_T$, is the product $\bar{R}\bar{H}$ for each month. The monthly radiation, S, is $\bar{H}_T$ multiplied by the number of days in each month. These results are displayed in Table A2.

Resumen—Este artículo concierne a sistemas de calentamiento solar de agua y ambiente para residencias. Se describe un modelo de simulación capaz de estimar el comportamiento térmico a largo plazo de sistemas de calentamiento solar. Se investiga la cantidad de datos meteorológicos requeridos por la simulación en función de la estimación a largo plazo del comportamiento. Se usa la información obtenida de muchas simulaciones para desarrollar un procedimiento de diseño general para sistemas de calentamiento solar. El resultado es un simple método gráfico que requiere datos promedio mensuales meteorológicos que los arquitectos e ingenieros térmicos pueden usar en el diseño de sistemas de calentamiento solar económicos. En el Apéndice se dá el método de estimación del promedio mensual de radiación sobre superficies inclinadas.

Résumé—Cet article concerne la conception des systèmes de chauffage solaire d'ambiance ou d'eau, destinés aux utilisations résidentielles. On y décrit une simulation permettant d'estimer les performances à long terme des systèmes de chauffage solaires. On étudie la quantité de données météorologiques nécessaire à la simulation des performances à long terme. Les informations déduites de nombreuses simulations sont utilisées pour développer un procédé général de conception des systèmes de chauffage solaire. Le résultat en est une méthode graphique simple nécessitant les données météorologiques moyennes mensuelles et qui peut être employée par architectes ou ingénieurs thermiciens pour concevoir des systèmes de chauffage solaire économiques. Une méthode d'estimation du rayonnement moyen mensuel sur des plans inclinés est fournie en annexe.